Title	Cellular ROS imaging with hydro-Cy3 dye is strongly influenced by mitochondrial membrane potential
Author(s)	Zhdanov, Alexander V.; Aviello, Gabriella; Knaus, Ulla G.; Papkovsky, Dmitri B.
Publication date	2016-11-04
Original citation	Zhdanov, A. V., Aviello, G., Knaus, U. G. and Papkovsky, D. B. (2017) 'Cellular ROS imaging with hydro-Cy3 dye is strongly influenced by mitochondrial membrane potential', Biochimica et Biophysica Acta (BBA) - General Subjects, 1861(2), pp. 198-204. doi:10.1016/j.bbagen.2016.10.023
Type of publication	Article (peer-reviewed)
Link to publisher's version	http://dx.doi.org/10.1016/j.bbagen.2016.10.023 Access to the full text of the published version may require a subscription.
Rights	**© 2016, Elsevier. This manuscript version is made available under the CC-BY-NC-ND 4.0 license** **http://creativecommons.org/licenses/by-nc-nd/4.0/** http://creativecommons.org/licenses/by-nc-nd/4.0/
Embargo information	Access to this item is restricted until 12 months after publication by the request of the publisher.
Embargo lift date	2017-11-04
Item downloaded from	http://hdl.handle.net/10468/3368

Accepted Manuscript

Cellular ROS Imaging with Hydro-Cy3 Dye is Strongly Influenced by Mitochondrial Membrane Potential

Alexander V. Zhdanov, Gabriella Aviello, Ulla G. Knaus, Dmitri B. Papkovsky

Please cite this article as: Alexander V. Zhdanov, Gabriella Aviello, Ulla G. Knaus, Dmitri B. Papkovsky, Cellular ROS Imaging with Hydro-Cy3 Dye is Strongly Influenced by Mitochondrial Membrane Potential, *BBA - General Subjects* (2016), doi:10.1016/j.bbagen.2016.10.023

Cellular ROS Imaging with Hydro-Cy3 Dye is Strongly Influenced by Mitochondrial Membrane Potential

Alexander V. Zhdanov[1], Gabriella Aviello[2], Ulla G. Knaus[2] and Dmitri B. Papkovsky[1]

[1] School of Biochemistry & Cell Biology, University College Cork, Cork, Ireland
[2] School of Medicine, Conway Institute, University College Dublin, Dublin, Ireland.

Running title: Hydro-Cy3 dynamics depend on mitochondrial polarisation

Corresponding author: Alexander V. Zhdanov, Cavanagh Pharmacy Building, University College Cork, College Road, Cork, Ireland. Email: a.zhdanov@ucc.ie, Tel: +353214901687

Key words: Key words: ROS probes, hydrocyanines, hydro-Cy3, mitochondrial membrane potential, live cell imaging

Abstract

Background

Hydrocyanines are widely used as fluorogenic probes to monitor reactive oxygen species (ROS) generation in cells. Their brightness, stability to autoxidation and photobleaching, large signal change upon oxidation, pH independence and red / near infrared emission are particularly attractive for imaging ROS in live tissue.

Methods

Using confocal fluorescence microscopy we have examined an interference of mitochondrial membrane potential ($\Delta\Psi$m) with fluorescence intensity and localisation of a commercial hydro-Cy3 probe in respiring and non-respiring colon carcinoma HCT116 cells.

Results

We found that the oxidised (fluorescent) form of hydro-Cy3 is highly homologous to the common $\Delta\Psi$m-sensitive probe JC-1, which accumulates and aggregates only in 'energised' negatively charged mitochondrial matrix. Therefore, hydro-Cy3 oxidised by hydroxyl and superoxide radicals tends to accumulate in mitochondrial matrix, but dissipates and loses brightness as soon as $\Delta\Psi$m is compromised. Experiments with mitochondrial inhibitor oligomycin and uncoupler FCCP, as well as a common ROS producer paraquat demonstrated that signals of the oxidised hydro-Cy3 probe rapidly and strongly decrease upon mitochondrial depolarisation, regardless of the rate of cellular ROS production.

Conclusions

While analysing ROS-derived fluorescence of commercial hydrocyanine probes, an accurate control of $\Delta\Psi$m is required.

General significance

If not accounted for, non-specific effect of mitochondrial polarisation state on the behaviour of oxidised hydrocyanines can cause artefacts and data misinterpretation in ROS studies.

1. Introduction

Reactive oxygen species (ROS) regulate key cellular processes, and therefore mechanisms of their production and signalling are under active research [1, 2]. However detection of highly reactive short-lived ROS, which are rapidly produced, converted and removed in the cells and extracellular space, is very challenging and requires specific probes and quantitative methods. One common approach is the use of redox based off/on probes which produce a characteristic fluorescent signal upon chemical reactions with particular ROS molecules. Advantages and disadvantages of various small molecule and genetically encoded ROS probes are discussed in [3-8].

Since their introduction in 2009, hydrocyanine probes have been used for detection of hydroxyl and superoxide radicals ($^{\bullet}OH$ and $O_2^{-\bullet}$) within cells and tissue [9-14]. Thus, hydro-Cy3 has been applied to study NADPH oxidase (NOX)-dependent redox signalling in the intestine [15-19], antioxidant defence mechanisms in human malignant mesothelioma cells [20], ROS generation in Caco-2 cells is response to bacterial invasion [21], the effects of leukemia inhibitory factor on ROS production in neural cells derived from human embryonic stem cells [22]. At the same time, mechanisms of hydrocyanine oxidation by $^{\bullet}OH$ and $O_2^{-\bullet}$ and the factors which can interfere with ROS detection using these dyes have not been studied in detail. Herein, we demonstrate that the oxidised hydro-Cy3 dye accumulates in polarised mitochondria, and its signal amplitude and localisation are strongly affected by mitochondrial membrane potential ($\Delta\Psi m$).

2. Methods

2.1. Chemicals and reagents

Lipofectamine[TM] 2000, OptiMEM I, potentiometric probes TMRM (tetramethylrhodamine, methyl ester) and JC-1 (5,5′,6,6′-tetrachloro-1,1′,3,3′-tetraethylbenzimidazolylcarbocyanine) were from Invitrogen Life Technologies (Carlsbad, CA and Dun Laoghaire, Ireland). RIPA buffer was from Thermo Fisher Scientific (Waltham, MA). ROSstar 550 (hydro-Cy3) probe [9] was from LI-COR Biosciences (Lincoln, NE, USA). GFP-tagged mitochondria targeting ROS probe HyPer-mito [23] was from Evrogen JSC (Moscow, Russia). Stainless Steel Minuten Pins (0.2 mm) were from Fine Science Tools (Foster City, CA, USA). Sylgard ® 184 silicon elastomer kit was from Dow Corning (Midland, MI). McCoy's 5A medium, collagen IV, poly-D-lysine (PDL), FCCP, oligomycin and all the other reagents were from Sigma-Aldrich. Plasticware was from Sarstedt (Ireland) and MatTek (Ashland, MA).

3

2.2. Tissue culture and cell treatment

Human colonic carcinoma wild type (HCT116 WT) cells were from the American Collections of Cell Cultures. Low respiring HCT116 deficient in the cytochrome c oxidase (COX) assembly protein SCO2 (Synthesis of Cytochrome c Oxidase 2) [24] were kindly provided by Professor P.M. Hwang (NIH). Cells were maintained in McCoy's medium supplemented with 10% FBS, 2 mM L-Glutamine, 100 U/ml penicillin / 100 μg/ml streptomycin (P/S), and 10 mM HEPES (pH 7.2) (complete McCoy's medium), in humidified atmosphere of 95% air and 5% CO_2 at 37°C. For fluorescence microscopy, cells were seeded at 2×10^4 (WT) and 1.6×10^4 ($SCO2^{-/-}$) cells on MatTek glass bottom dishes coated with a mixture of collagen IV and poly-D-lysine (0.007/0.003 mg/ml). Treatment with FCCP (mitochondrial uncoupler, 2 μM) and oligomycin (mitochondrial complex V inhibitor, 10 μM) were performed by adding 20× drug stock to the cells. Note that 2 μM FCCP does not affect plasma membrane potential in HCT116 cells (not shown).

2.3. Staining of cells with probes and confocal microscopy

For loading with hydro-Cy3, cells were washed with a low serum medium OptiMEM I, 5 μM probe was added to the cells in OptiMEM I medium 15 min before FCCP, oligomycin or mock (DMSO) treatment; then drugs were added and incubation was resumed for 15 min; finally the cells were washed from the probe, and drug treatment in complete McCoy's medium was continued for further 15 min prior to microscopy (scheme 1, end-point analysis). Alternatively, cells were washed with OptiMEM I, incubated with 5 μM probe in OptiMEM I for 30 min, transferred to complete McCoy's medium without the probe, and then imaged (scheme 2, kinetic analysis of the responses to drug treatment). Loading of the cells with mitochondrial membrane potential (ΔΨm)-sensitive probes TMRM (20 nM, non-quenching concentration) [25] and JC-1 (1 μM) was performed in McCoy's medium for 30 min; 20 nM concentration of TMRM was maintained in the medium during the measurement. The plasmid encoding HyPer-mito was delivered to the cells by Lipofectamine 2000 transfection in OptiMEM I medium, according to manufacturer's protocol.

Live cell imaging was conducted on an Olympus FV1000 confocal laser-scanning microscope with controlled CO_2, humidity and temperature. HyPer-mito was excited at 405 (1.5-2.5% of the maximal laser power) and 488 nm (2.5-10% laser power); emission was collected at 500-550 nm; the ratio of emission signals upon the dual excitation (488/405 nm ratio) was then

4

calculated. Cy3 and TMRM were excited at 543 nm (5% of laser power), emission was collected at 560-600 nm. Double excitation / emission was used for JC-1 probe (488/500-540 nm for non-aggregated probe and 543/560-620 nm for J-aggregates). Acquisition of each spectral signal was done in sequential laser mode with emission bands adjusted to avoid spectral overlap. Fluorescence and differential interference contrast (DIC) images were collected with a 60X oil immersion objective in 2-8 planes using 0.5 µm steps (80-100 µm aperture). The resulting single plain (DIC) and z-stacked images were analysed using FV1000 Viewer (Olympus), Adobe Photoshop and Illustrator software.

2.4. ROS imaging in mouse colon tissue

C57BL/6 mice (Harlan, UK) were handled and euthanized as described [26], in accordance with the regulations and guidelines of the Irish Department of Health; protocols were approved by the University College Cork Animal Experimentation Ethics Committee. The distal colon was dissected, opened along the mesenteric border and pinned to the bottom of Sylgard-coated 3.5 cm^2 Petri dishes with the mucosal side facing up. Staining with hydro-Cy3 (15 µM, 70 min at 37°C) was conducted in Krebs buffer supplemented with 2% BSA, in a humidified CO_2 incubator. Stained tissue was washed with Krebs buffer supplemented with 2 mM L-glutamine and 0.1 mM atropine and imaged on a confocal upright fluorescent microscope AxioExaminer Z1 equipped with 20×/1.0 W-Plan-Apochromat water immersion objective (Carl Zeiss), using SPCM software (Becker & Hickl) [26]. Images of Cy3 were collected in 3 focal planes at 10, 20 and 30 µm depth from the mucosal surface (0.5 mm aperture). The dye was excited with SC400-4 laser (Fianium, UK) at 540 nm; emission was collected with a 561 nm longpass / 545-625 nm bandpass filter pair. 2D matrices of Cy3 intensity data (256×256 pixel) for each measurement were exported to Excel. Stacked ROS images were reconstructed using ImageJ program.

2.5. Analysis of Cy3 diffusion from the cells

HCT116 cells (WT) were seeded at $3×10^4$ cells per well on a standard 96-well plate coated with a mixture of collagen IV and poly-D-lysine. Staining with hydro-Cy3 was performed as above (for 1 h). After washing with complete McCoy's medium, cells were incubated for 30 min (37°C in CO_2 incubator) in complete McCoy's medium or the same medium containing FCCP (2 µM) or FCCP / KCl (70 mM), 30 µl final volume. Non-stained cells were used as negative control. In parallel, lysates of stained and non-stained cell were prepared using

standard RIPA buffer (30 μl per well). After incubation the supernatants, cells (in the same volume of complete McCoy's medium) and cell lysates were collected and analysed on a multi-mode plate reader FlexStation 3 (Molecular Devices, Sunnyvale, CA), at 544 nm excitation / 590 nm emission.

2.6. Statistical Analysis

Statistical analysis was performed using the results of 3-4 independent experiments. P values of ≤ 0.05 were deemed as statistically significant. The differences in Cy3, TMRM and HyPer-mito signals upon treatment, as well as Cy3 diffusion from the cells were evaluated using non-parametrical Mann-Whitney U-test and presented graphically as mean±SEM or mean±SD (both normalised to the values before treatment or after mock treatment both 1 a.u.).

1. Results and Discussion

In human cancer HCT116 cell line deficient in SCO2 protein (SCO2$^{-/-}$ cells), mitochondrial respiration is negligible [27]. Compared to WT counterparts, SCO2$^{-/-}$ cells with a malfunctioning electron transport chain have been shown to over-generate ROS, mainly by the cytoplasmic NADPH oxidases [28]. However in that study a probe with arguable specificity to ROS (DCFDA) [6] was used, which made the result rather ambiguous. Analysing TMRM dynamics upon oligomycin treatment, we found that in SCO2$^{-/-}$ cells, the F1Fo ATP synthase (complex V) is working in reverse mode in order to maintain partial (~80%) mitochondrial polarisation (not shown). We proposed that, by energising the mitochondria, complex V contributes to ROS production, and that inhibition of the reversed complex V with oligomycin, which causes $\Delta\Psi$m depolarisation [29], might reduce ROS levels in these cells.

We reasoned that upon inhibition of complex V, mitochondrial ROS levels should be most affected. To visualise this and quantify the differences between oligomycin-treated and control cells, we transfected them with the plasmid encoding HyPer-mito (detects mitochondrial H_2O_2) and loaded them with cell-permeable hydro-Cy3, which reacts with $^\bullet$OH and $O_2^{-\bullet}$ [9]. Treatment with an uncoupler FCCP which depolarises $\Delta\Psi$m, was used as a positive control. Confocal microscopy revealed not only an expected decrease in HyPer-mito signals (by ~40%, Supplemental Fig. 1), but also a marked decrease in Cy3 signals in SCO2$^{-/-}$ cells treated with oligomycin or FCCP, as well as in WT cells treated with FCCP (Fig. 1). Surprisingly, without FCCP treatment, Cy3 staining was slightly brighter in WT than SCO2$^{-/-}$ cells. Moreover, Cy3 showed typical mitochondrial pattern: it co-localised well with HyPer-mito (90-95% signal overlap, Fig. 2A, B), which has a duplicated mitochondria-targeting sequence derived from the subunit VIII of human cytochrome C oxidase [30].

It is important to note that limited resolution of standard confocal microscopy does not allow to clearly distinguish between mitochondrial and cytosolic localisation of the Cy3 dye in live tissue. In particular, none of the studies of intestinal ROS levels using hydro-Cy3 (regardless of the probe delivery method or ROS type) unambiguously showed its distribution in individual cells [15, 17, 19, 21], meaning that mitochondrial accumulation of the oxidised probes could be simply overlooked. While imaging ROS in mouse colon tissue, we also observed whole cytosol rather than mitochondrial Cy3 staining of the colonocytes (Fig. 2C) [31].

A hydro-Cy3 analogue, hydro-Cy5 has been previously reported to detect an increase in mitochondrial ROS production in neuronal cells treated with amyloid β-peptide [14]. Therefore we initially thought that Cy3 signals reflected the levels of $^{\bullet}OH$ and $O_2^{-\bullet}$ produced mainly in the matrix of HCT116 cells. However, careful analysis of cyanine dye chemical structure and experimental data overturned such interpretation.

Indeed, the oxidised (fluorescent) form of hydro-Cy3 is highly homologous to the common (although also criticised [32]) $\Delta\Psi m$-sensitive cationic cyanine probes JC-1 and $DiOC_N(3)$ (N < 7) (Fig. 3). JC-1 accumulates and aggregates only in 'energised' negatively charged mitochondrial matrix [33]. Hence we deducted that hydro-Cy3 molecule, when oxidised by ROS at different cellular locations, gains a positive charge and accumulates inside the matrix proportionally to mitochondrial polarisation. Hydro-Cy3 (MW = 768) can penetrate across the outer mitochondrial membrane and get oxidised in the intermembrane space by the short-lived $^{\bullet}OH$ and $O_2^{-\bullet}$ produced in the matrix. Therefore, a decrease in Cy3 signal observed in cells with depolarised mitochondria could be due to inhibited ROS production, compromised influx of the oxidised dye into the matrix, or both. We ruled out the contribution of matrix acidification to Cy3 signal (Cy3 is pH-insensitive) and conversion of Cy3 back to non-fluorescent hydro-Cy3 (this requires stringent conditions, such as $NaBH_4$ and methanol [9]).

To study the mechanism of Cy3 accumulation in the mitochondria, we pre-loaded WT and $SCO2^{-/-}$ cells with hydro-Cy3 and monitored its Cy3 signal upon double treatment of cells with FCCP/oligomycin [34]. Strong decrease and de-localisation of Cy3 signal were observed in both cell lines (exemplified by $SCO2^{-/-}$ cells in Fig. 4), suggesting that the probe was released from the mitochondria after $\Delta\Psi m$ depolarisation (Fig. 4A), similar to JC-1 (Fig. 4B). TMRM probe signal also decreased ~3 fold in $SCO2^{-/-}$ (Fig. 4B) and 5-6 fold in WT cells (not shown). Such strong effect of $\Delta\Psi m$ on localisation and brightness of the probe proves that Cy3 signals do not reflect the actual rates and sites of $^{\bullet}OH$ and $O_2^{-\bullet}$ production in the cell. As a result, ROS levels in $SCO2^{-/-}$ cells could be largely underestimated, and mitochondria wrongly identified as the main source of ROS.

To test whether Cy3 is retained in the cytosol upon mitochondrial depolarisation or diffuses to the extracellular space, we examined probe concentration in the medium surrounding cells treated with DMSO (Mock), FCCP (2 μM) and FCCP / KCL (70 mM); the latter double treatment depolarises both $\Delta\Psi m$ and $\Delta\Psi p$ (plasma membrane potential). WT cells were selected for the analysis, because they demonstrated better Cy3 staining (Fig. 1). Our results suggested that the oxidised probe diffuses to the extracellular space even from the 'resting'

cells, and the diffusion increases upon depolarisation of the $\Delta\Psi$m (Supplemental Fig. 2). Further analysis of the dynamics and mechanisms of probe diffusion from the cells was outside the scope of this study.

Finally, we compared the effect of $\Delta\Psi$m depolarisation on Cy3 signal in cells treated with a common ROS producer paraquat [35]. This herbicide converts O_2 into $O_2^{\bullet-}$ in the presence of electron donors NAD(P)H, which are elevated in $SCO2^{-/-}$ cells [28]. We observed a significant increase in Cy3 signal in $SCO2^{-/-}$ cells incubated with paraquat, compared to mock (Fig. 5). Upon $\Delta\Psi$m depolarisation, Cy3 signals rapidly decreased. In $SCO2^{-/-}$ cells pre-incubated with oligomycin, treatment with paraquat did not affect Cy3 signal (not shown). Note that paraquat treatment did not affect $\Delta\Psi$m polarisation (Supplemental Fig. 3). These data confirm that hydro-Cy3 does strongly respond to the changes in O_2^- levels, but the dependence of Cy3 on $\Delta\Psi$m impedes quantitative analysis of ROS in cells with depolarised mitochondria.

Overall, prominent cross-sensitivity to $\Delta\Psi$m of oxidised hydro-Cy3 probe has to be factored in when using it for cellular $^{\bullet}OH$ and $O_2^{\bullet-}$ analysis. Hydrocyanine probes should be used with care, particularly while studying cells and tissues with compromised mitochondrial function or processes affecting mitochondrial polarisation state. Otherwise, these probes cannot inform unambiguously on the quantity of ROS and their main production sites.

Figure Legends

Figure 1. Effects of $\Delta\Psi$m depolarisation on the fluorescence of the oxidised hydro-Cy3. A. Cy3 signals in HCT116 $SCO2^{-/-}$ (left panel) and WT cells (right panel) treated with DMSO (Mock) or with a mitochondrial uncoupler FCCP (2 μM) for 30 min. B. Cy3 signals in $SCO2^{-/-}$ cells treated with oligomycin (OM, 10 μM) for 30 min. All images are stacks of 8 confocal planes taken with 0.5 μm step. C. Quantitative analysis of results (A-B). Error bars show SEM. Asterisks demonstrate significant difference ($p<0.01$, U-test). Scale bar is 50 μm.

Figure 2. Intracellular localisation of Cy3 dye. A. Co-localisation of Cy3 with genetically encoded GFP-tagged mitochondrial H_2O_2 probe HyPer-mito; stacks of 5 confocal images taken with 0.5 μm step. Signal overlap is 92-94%. A single HCT116 $SCO2^{-/-}$ cells is shown. Scale bar is 20 μm. B. Line profile analysis of the two fluorescence spectra, shown in (A). C.

9

Mouse colon tissue stained with hydro-Cy3; stack of 3 images taken with 10 μm step. Scale bar is 100 μm.

Figure 3. Chemical structures of hydro-Cy3 probe and ΔΨm-dependent Cy3, JC-1 and DiOC$_N$(3) dyes. A. Changes in hydro-Cy3 structure induced by ROS. B. Structures of cationic cyanine probes JC-1 and DiOC$_N$(3). Positive charge at nitrogen atom is shown in red. C. Proposed mechanism of oxidised dye (Cy3, positively charged) accumulation in negatively charged mitochondrial matrix.

Figure 4. Cy3, JC-1 and TMRM signal kinetics upon ΔΨm depolarisation in HCT116 SCO2$^{-/-}$ cells. A. Stacks of 3 confocal images of Cy3 taken with 0.5 μm step before and 10 min after addition of FCCP (2 μM) and oligomycin (OM, 10 μM). Bottom panel: quantitative analysis of Cy3 response to the double treatment with FCCP/OM of SCO2$^{-/-}$ and WT cells. Error bars show SD. Asterisk demonstrates significant decrease ($p<0.01$, U-test). B. Responses of probes JC-1 (top) and TMRM (bottom) to FCCP/OM treatment. Note that J-aggregates in resting SCO2$^{-/-}$ cells are rarely formed, as their mitochondria are partially depolarised. Scale bar is 50 μm.

Figure 5. Effects of paraquat on Cy3 signals in the resting and FCCP treated SCO2$^{-/-}$ cells. A. Stacks of 6 confocal images of Cy3 taken with 0.5 μm step. Left panel shows an increase in Cy3 signals upon paraquat treatment (1 mM, 1 h); typical mitochondrial localisation is seen. Right panel: a decrease in Cy3 signals upon FCCP treatment (2 μM, 10 min). B. Quantitative analysis of the imaging data (A). Error bars show SEM. Asterisk demonstrates significant difference ($p<0.01$, U-test). Scale bar is 50 μm.

References

[1] D.B. Zorov, M. Juhaszova, S.J. Sollott, Mitochondrial reactive oxygen species (ROS) and ROS-induced ROS release, Physiological reviews, 94 (2014) 909-950.

[2] K.M. Holmstrom, T. Finkel, Cellular mechanisms and physiological consequences of redox-dependent signalling, Nat Rev Mol Cell Biol, 15 (2014) 411-421.

[3] S.I. Dikalov, D.G. Harrison, Methods for detection of mitochondrial and cellular reactive oxygen species, Antioxidants & redox signaling, 20 (2014) 372-382.

[4] A.J. Meyer, T.P. Dick, Fluorescent protein-based redox probes, Antioxidants & redox signaling, 13 (2010) 621-650.

[5] X. Chen, X. Tian, I. Shin, J. Yoon, Fluorescent and luminescent probes for detection of reactive oxygen and nitrogen species, Chemical Society Reviews, 40 (2011) 4783-4804.

[6] B. Kalyanaraman, V. Darley-Usmar, K.J.A. Davies, P.A. Dennery, H.J. Forman, M.B. Grisham, G.E. Mann, K. Moore, L.J. Roberts Ii, H. Ischiropoulos, Measuring reactive oxygen and nitrogen species with fluorescent probes: challenges and limitations, Free Radical Biology and Medicine, 52 (2012) 1-6.

[7] J.F. Woolley, J. Stanicka, T.G. Cotter, Recent advances in reactive oxygen species measurement in biological systems, Trends in Biochemical Sciences, 38 (2013) 556-565.

[8] D.S. Bilan, V.V. Belousov, HyPer family probes: state of the art, Antioxidants & redox signaling, (2015).

[9] K. Kundu, S.F. Knight, N. Willett, S. Lee, W.R. Taylor, N. Murthy, Hydrocyanines: a class of fluorescent sensors that can image reactive oxygen species in cell culture, tissue, and in vivo, Angewandte Chemie International Edition, 48 (2009) 299-303.

[10] P. Goodson, A. Kumar, L. Jain, K. Kundu, N. Murthy, M. Koval, M.N. Helms, Nadph oxidase regulates alveolar epithelial sodium channel activity and lung fluid balance in vivo via O2− signaling, American Journal of Physiology-Lung Cellular and Molecular Physiology, 302 (2012) L410-L419.

[11] S. Selvam, K. Kundu, K.L. Templeman, N. Murthy, A.J. García, Minimally invasive, longitudinal monitoring of biomaterial-associated inflammation by fluorescence imaging, Biomaterials, 32 (2011) 7785-7792.

[12] K. Kundu, S.F. Knight, S. Lee, W.R. Taylor, N. Murthy, A Significant Improvement of the Efficacy of Radical Oxidant Probes by the Kinetic Isotope Effect, Angewandte Chemie International Edition, 49 (2010) 6134-6138.

[13] S. Magalotti, T.P. Gustafson, Q. Cao, D.R. Abendschein, R.A. Pierce, M.Y. Berezin, W.J. Akers, Evaluation of inflammatory response to acute ischemia using near-infrared fluorescent reactive oxygen sensors, Molecular imaging and biology, 15 (2013) 423-430.

[14] Y. Jiao, Y. Zhang, Y. Wei, Z. Liu, W. An, M. Guo, Direct Observation of Internalization and ROS Generation of Amyloid β-Peptide in Neuronal Cells at Subcellular Resolution, ChemBioChem, 13 (2012) 2335-2338.

[15] G. Leoni, A. Alam, P.-A. Neumann, J.D. Lambeth, G. Cheng, J. McCoy, R.S. Hilgarth, K. Kundu, N. Murthy, D. Kusters, Annexin A1, formyl peptide receptor, and NOX1 orchestrate epithelial repair, The Journal of clinical investigation, 123 (2013) 443.

[16] R.M. Jones, L. Luo, C.S. Ardita, A.N. Richardson, Y.M. Kwon, J.W. Mercante, A. Alam, C.L. Gates, H. Wu, P.A. Swanson, Symbiotic lactobacilli stimulate gut epithelial proliferation via Nox-mediated generation of reactive oxygen species, The EMBO journal, 32 (2013) 3017-3028.

[17] C.C. Wentworth, A. Alam, R.M. Jones, A. Nusrat, A.S. Neish, Enteric commensal bacteria induce extracellular signal-regulated kinase pathway signaling via formyl peptide receptor-dependent redox modulation of dual specific phosphatase 3, Journal of Biological Chemistry, 286 (2011) 38448-38455.

[18] A. Alam, G. Leoni, C.C. Wentworth, J.M. Kwal, H. Wu, C.S. Ardita, P.A. Swanson, J.D. Lambeth, R.M. Jones, A. Nusrat, Redox signaling regulates commensal-mediated mucosal homeostasis and restitution and requires formyl peptide receptor 1, Mucosal immunology, 7 (2014) 645-655.

[19] P.A. Swanson, A. Kumar, S. Samarin, M. Vijay-Kumar, K. Kundu, N. Murthy, J. Hansen, A. Nusrat, A.S. Neish, Enteric commensal bacteria potentiate epithelial restitution via reactive oxygen species-mediated inactivation of focal adhesion kinase phosphatases, Proceedings of the National Academy of Sciences, 108 (2011) 8803-8808.

[20] K. Newick, B. Cunniff, K. Preston, P. Held, J. Arbiser, H. Pass, B. Mossman, A. Shukla, N. Heintz, Peroxiredoxin 3 is a redox-dependent target of thiostrepton in malignant mesothelioma cells, PloS one, 7 (2012) e39404.

[21] C.S. Ardita, J.W. Mercante, Y.M. Kwon, L. Luo, M.E. Crawford, D.N. Powell, R.M. Jones, A.S. Neish, Epithelial adhesion mediated by pilin SpaC is required for Lactobacillus rhamnosus GG-induced cellular responses, Applied and environmental microbiology, 80 (2014) 5068-5077.

[22] A. Majumder, S. Banerjee, J.A. Harrill, D.W. Machacek, O. Mohamad, M. Bacanamwo, W.R. Mundy, L. Wei, S.K. Dhara, S.L. Stice, Neurotrophic effects of leukemia inhibitory factor on neural cells derived from human embryonic stem cells, Stem Cells, 30 (2012) 2387-2399.

[23] V.V. Belousov, A.F. Fradkov, K.A. Lukyanov, D.B. Staroverov, K.S. Shakhbazov, A.V. Terskikh, S. Lukyanov, Genetically encoded fluorescent indicator for intracellular hydrogen peroxide, Nature methods, 3 (2006) 281-286.

[24] T. Matsumoto, P.Y. Wang, W. Ma, H.J. Sung, S. Matoba, P.M. Hwang, Polo-like kinases mediate cell survival in mitochondrial dysfunction, Proc Natl Acad Sci U S A, 106 (2009) 14542-14546.

[25] D.G. Nicholls, Simultaneous monitoring of ionophore-and inhibitor-mediated plasma and mitochondrial membrane potential changes in cultured neurons, Journal of Biological Chemistry, 281 (2006) 14864-14874.

[26] A.V. Zhdanov, I.A. Okkelman, F.W. Collins, S. Melgar, D.B. Papkovsky, A novel effect of DMOG on cell metabolism: direct inhibition of mitochondrial function precedes HIF target gene expression, Biochimica et Biophysica Acta (BBA)-Bioenergetics, 1847 (2015) 1254-1266.

[27] S. Matoba, J.-G. Kang, W.D. Patino, A. Wragg, M. Boehm, O. Gavrilova, P.J. Hurley, F. Bunz, P.M. Hwang, p53 regulates mitochondrial respiration, Science, 312 (2006) 1650-1653.

[28] H.J. Sung, W. Ma, P.-y. Wang, J. Hynes, T.C. O'Riordan, C.A. Combs, J.P. McCoy Jr, F. Bunz, J.-G. Kang, P.M. Hwang, Mitochondrial respiration protects against oxygen-associated DNA damage, Nature communications, 1 (2010) 5.

[29] I. Scott, D. Nicholls, Energy transduction in intact synaptosomes. Influence of plasma-membrane depolarization on the respiration and membrane potential of internal mitochondria determined in situ, Biochem. J, 186 (1980) 21-33.

[30] R. Rizzuto, M. Brini, P. Pizzo, M. Murgia, T. Pozzan, Chimeric green fluorescent protein as a tool for visualizing subcellular organelles in living cells, Current biology, 5 (1995) 635-642.

[31] G. Pircalabioru, G. Aviello, M. Kubica, A. Zhdanov, M.-H. Paclet, L. Brennan, R. Hertzberger, D. Papkovsky, B. Bourke, U.G. Knaus, Defensive Mutualism Rescues NADPH Oxidase Inactivation in Gut Infection, Cell host & microbe, 19 (2016) 651-663.

[32] D.G. Nicholls, Fluorescence measurement of mitochondrial membrane potential changes in cultured cells, Mitochondrial Bioenergetics: Methods and Protocols, (2012) 119-133.

[33] S.T. Smiley, M. Reers, C. Mottola-Hartshorn, M. Lin, A. Chen, T.W. Smith, G. Steele, L.B. Chen, Intracellular heterogeneity in mitochondrial membrane potentials revealed by a J-aggregate-forming lipophilic cation JC-1, Proceedings of the National Academy of Sciences, 88 (1991) 3671-3675.

[34] D.G. Nicholls, M.W. Ward, Mitochondrial membrane potential and neuronal glutamate excitotoxicity: mortality and millivolts, Trends in Neurosciences, 23 (2000) 166-174.

[35] J.S. Bus, J.E. Gibson, Paraquat: model for oxidant-initiated toxicity, Environmental health perspectives, 55 (1984) 37.
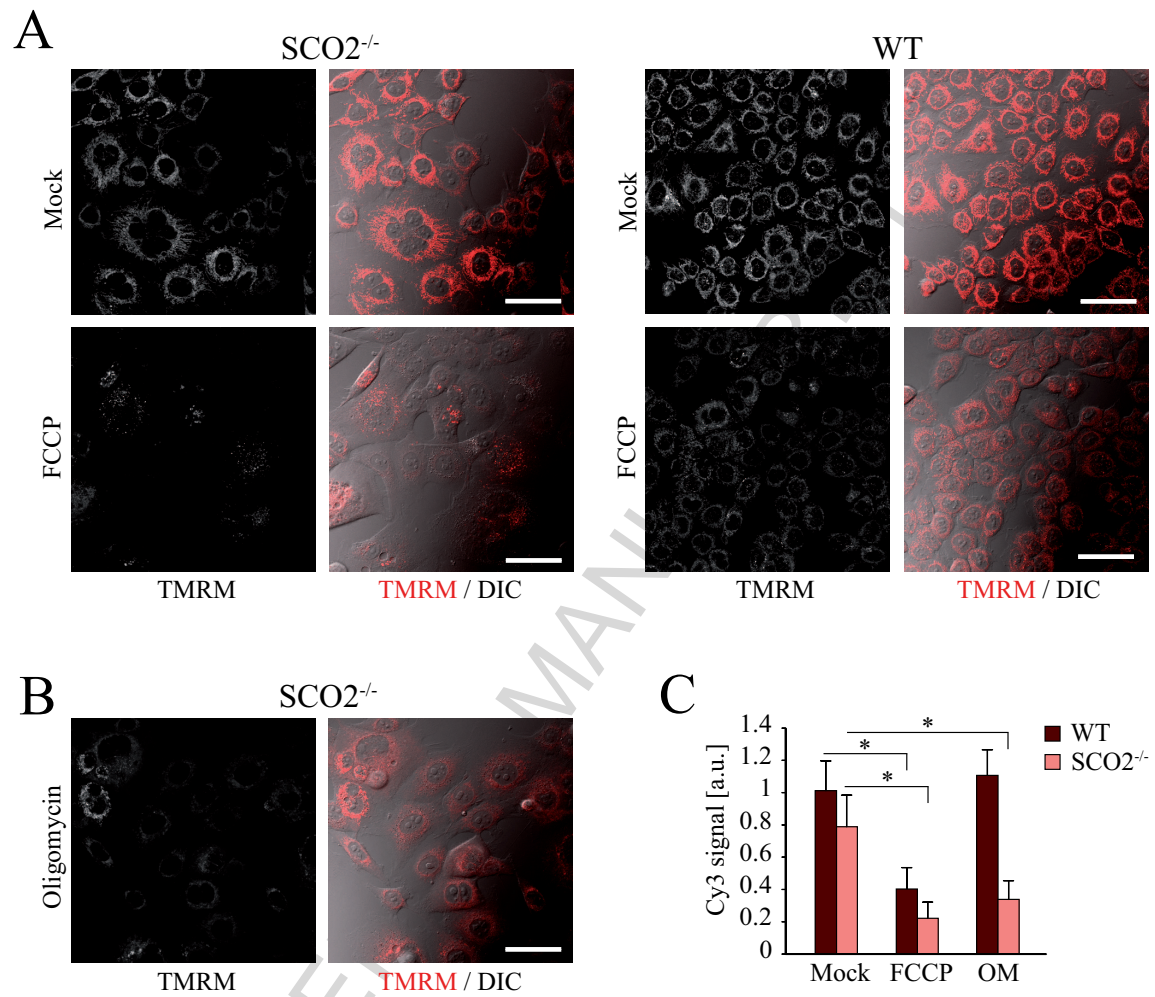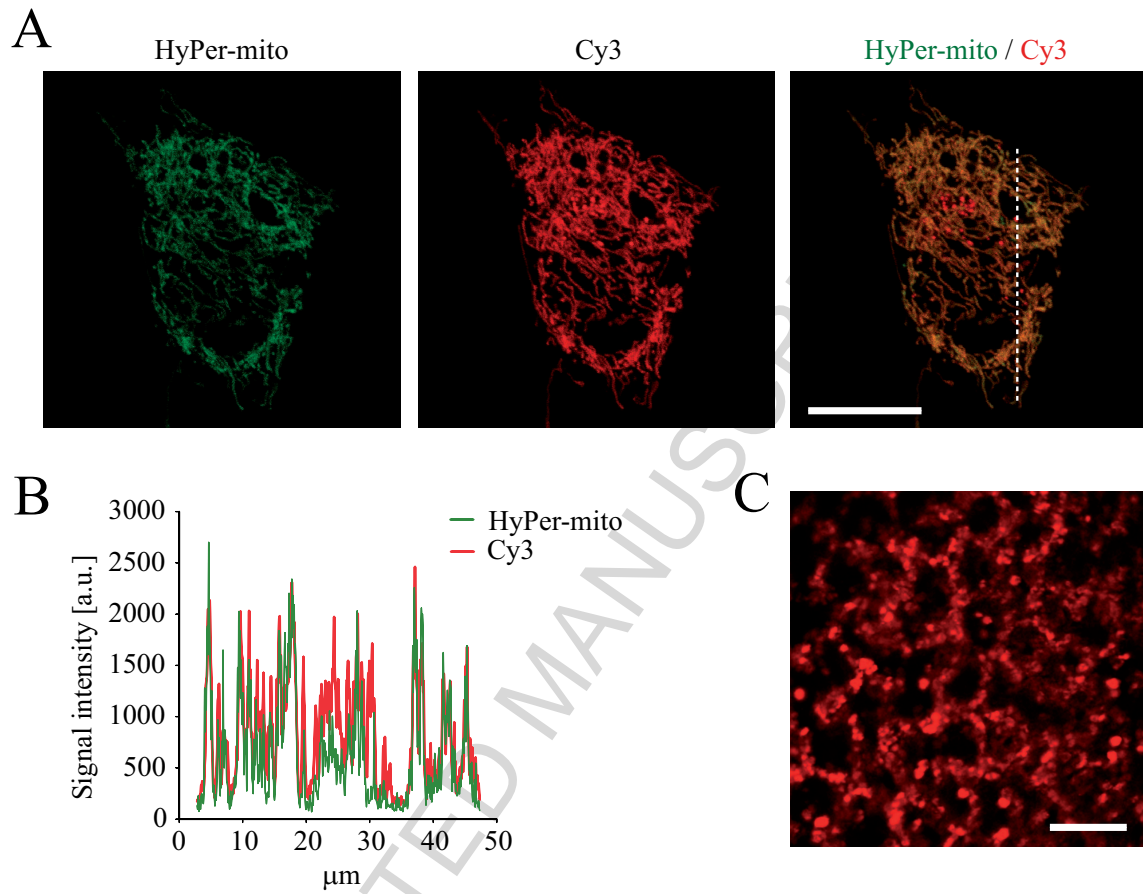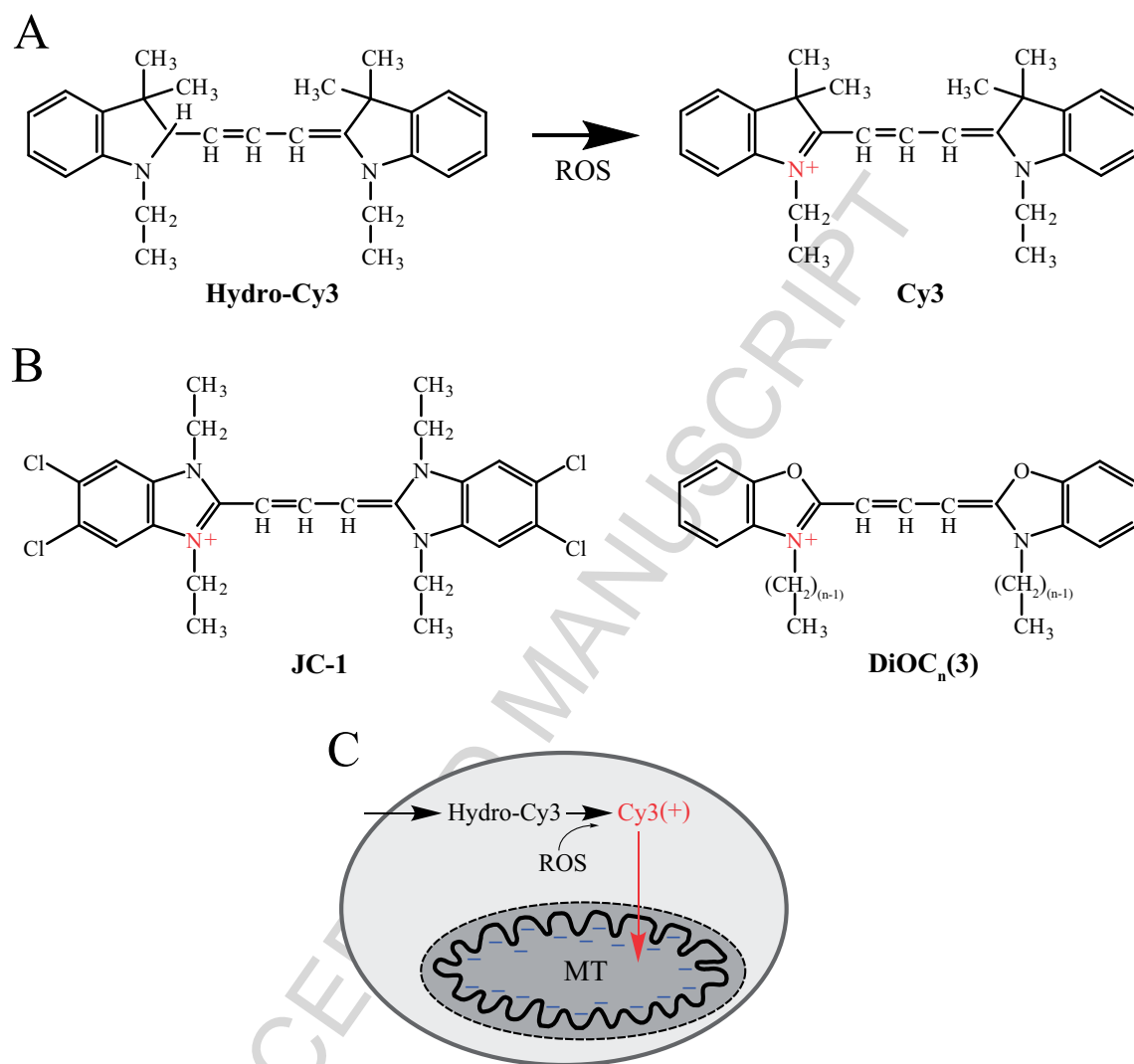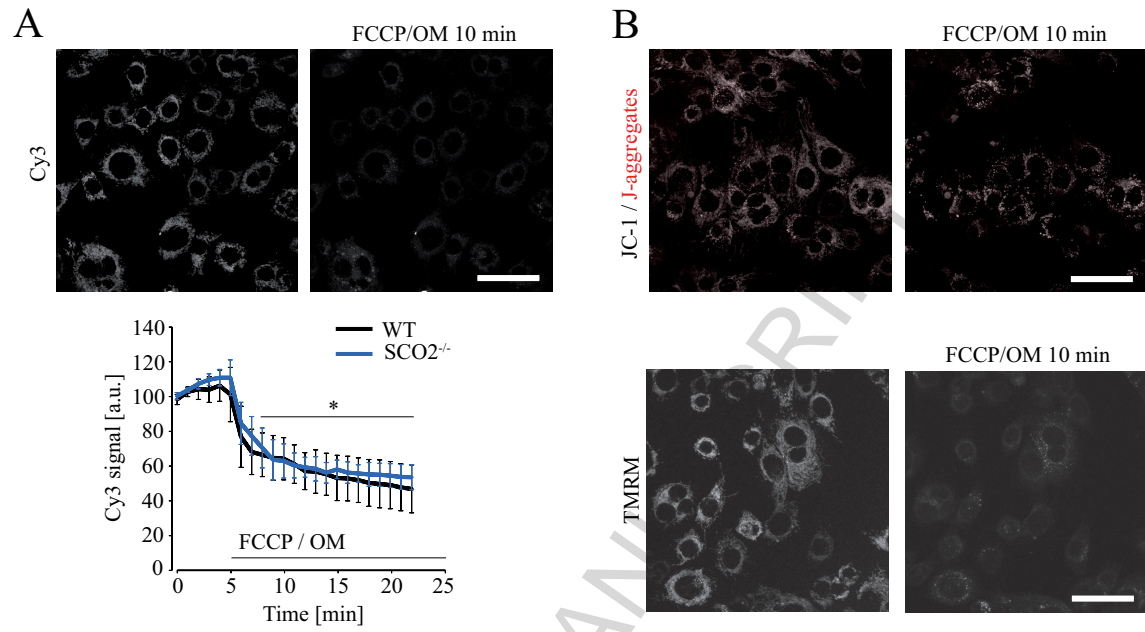
Figure 1

A

HyPer-mito | Cy3 | HyPer-mito / Cy3

B

C

Figure 2

A

Hydro-Cy3 → (ROS) → **Cy3**

B

JC-1

DiOC$_n$(3)

C

Hydro-Cy3 → Cy3(+)

ROS

MT

Figure 3

A

B

Figure 4

A
SCO2$^{-/-}$ cells before FCCP treatment   10 min FCCP

Mock

Paraquat

Cy3   Cy3 / DIC   Cy3   Cy3 / DIC

B

Figure 5

Graphical Abstract

Cell

Hydro-Cy3 → **Cy3(+)**

ROS

Mitochondria

Uncoupling

Cy3 accumulates in polarised mitochondria

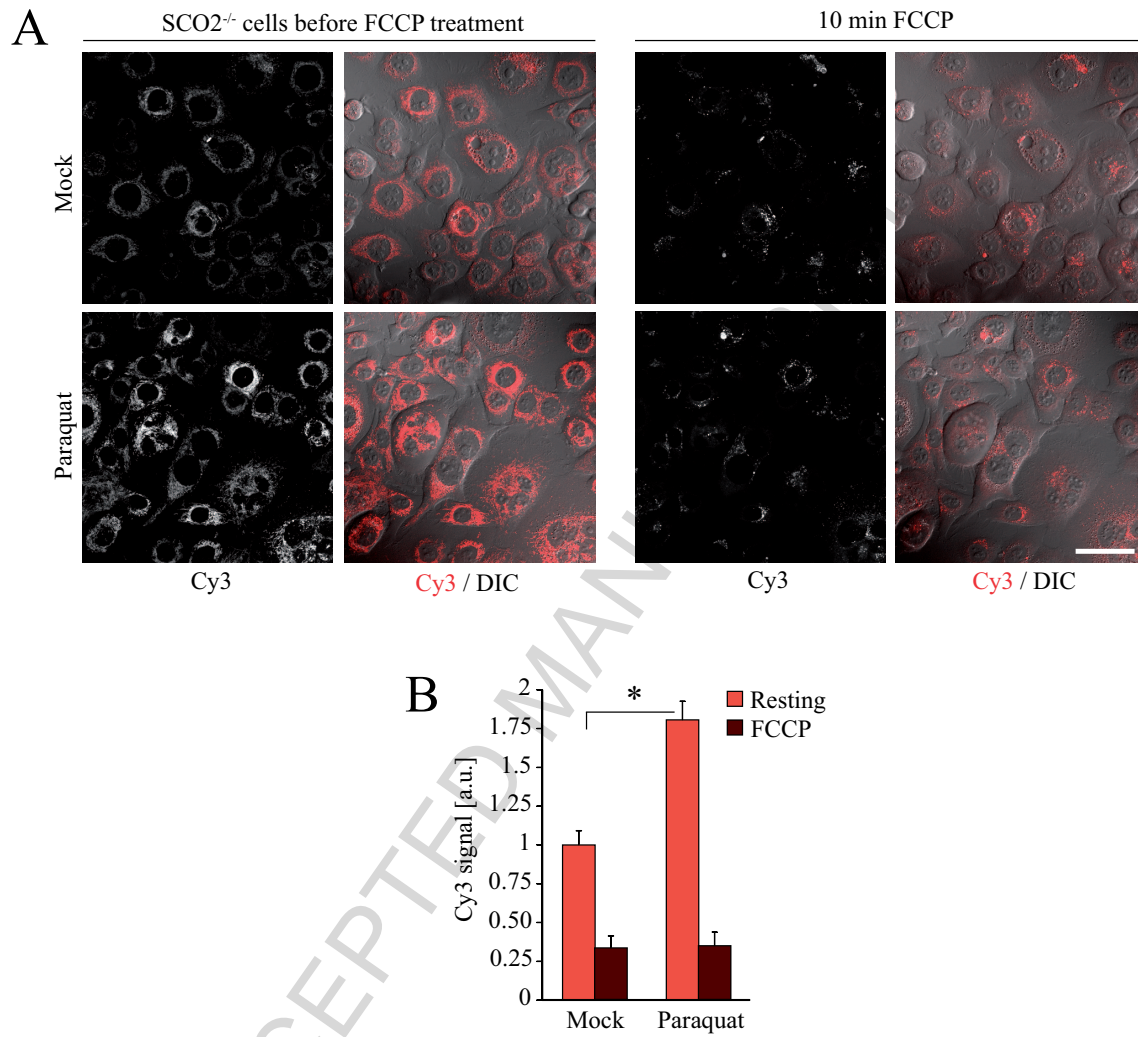CAUTION: Potential data misinterpretation!

Signal dissipates from depolarised mitochondria
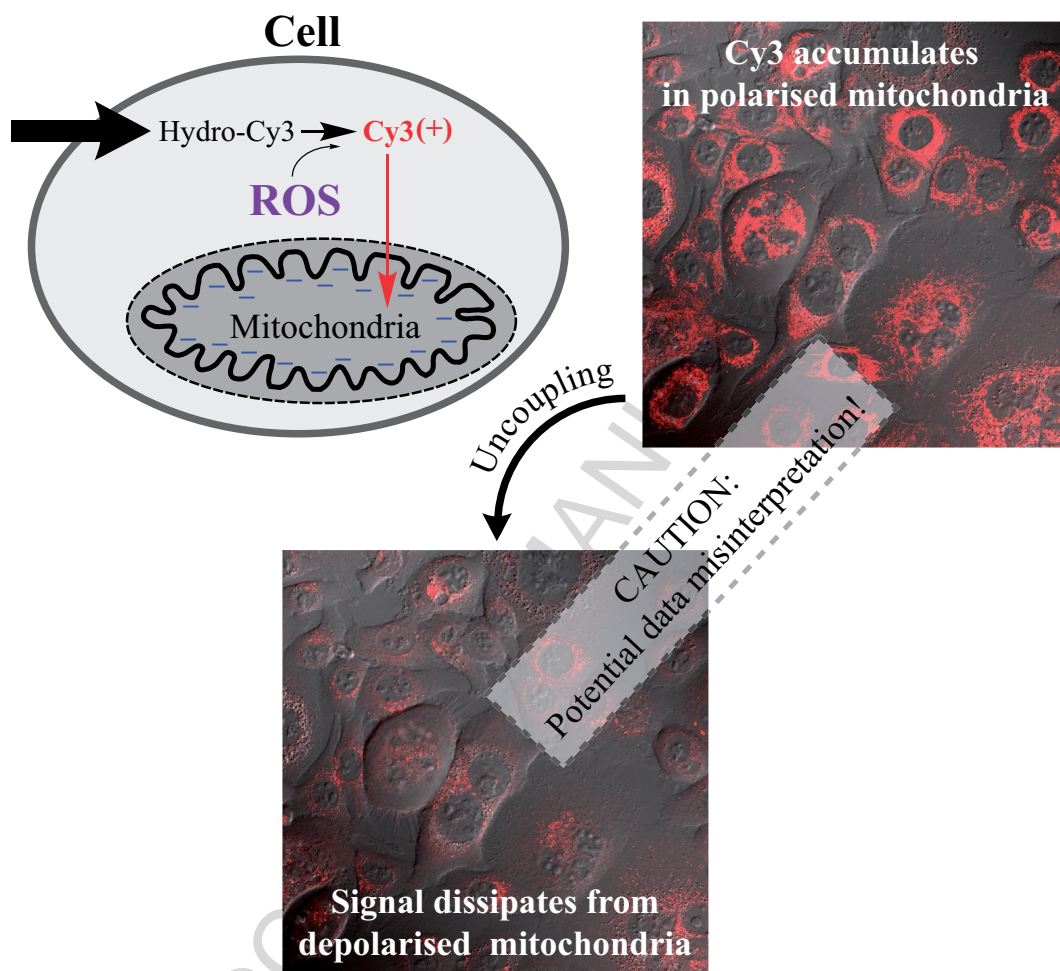
Highlights

A critical drawback of common ROS probes hydrocyanines is described

When oxidised by ROS, intracellular hydro-Cy3 accumulates in polarised mitochondria

Cy3 signal dissipates and loses brightness upon mitochondrial depolarisation

Cy3 may misinform on the quantity of ROS and their main production sites in the cell

Control of mitochondrial polarisation state is mandatory when using hydrocyanines